

LIGO Laboratory / LIGO Scientific Collaboration

LIGO-T080067-04-D

10/22/2008

Protecting installed core optics from particulates

M. E. Zucker

Distribution of this document:
Detector Revision Technical Review Board

This is an internal working note
of the LIGO Laboratory.

California Institute of Technology
LIGO Project – MS 18-34
1200 E. California Blvd.
Pasadena, CA 91125
Phone (626) 395-2129
Fax (626) 304-9834
E-mail: info@ligo.caltech.edu

Massachusetts Institute of Technology
LIGO Project – NW17-161
175 Albany St
Cambridge, MA 02139
Phone (617) 253-4824
Fax (617) 253-7014
E-mail: info@ligo.mit.edu

LIGO Hanford Observatory
P.O. Box 1970
Mail Stop S9-02
Richland WA 99352
Phone 509-372-8106
Fax 509-372-8137

LIGO Livingston Observatory
P.O. Box 940
Livingston, LA 70754
Phone 225-686-3100
Fax 225-686-7189

<http://www.ligo.caltech.edu/>

1. Scope

Advanced LIGO optics are vulnerable to particulate contamination in fabrication and during and after vessel installation, potentially limiting interferometer performance. Tolerable contamination levels, resulting environmental requirements, and methods for achieving and maintaining adequate conditions are developed and discussed.

2. Requirements

Surface particles absorb and scatter power from the interferometer mode. Such losses limit recycling and signal cavity finesse, degrading shot-noise limited strain sensitivity. However, under anticipated AdL conditions, heating from absorbed power and phase noise from scattered light are expected to constrain allowable particulates more stringently.

Initial LIGO cleanliness requirements were developed by Weiss in 1988 (T880049). The following treatment incorporates data made available in the intervening 20 years and extends the domain of applicability to cases of interest for Advanced LIGO.

Scattering and absorption

Generalized Mie scattering by small particles is a rich field of study. For example, Figure 1 shows a calculated Mie cross-section for dielectric spheres as a function of parameter $q = \pi D/\lambda$ where D is the diameter and λ the wavelength.

As discussed below, mean particle diameters for a broad variety of contamination scenarios appear to cluster around $D \sim 1 \mu\text{m}$ ($q \sim 3$ for $\lambda = 1.06 \mu\text{m}$). The corresponding area-weighted distributions peak between $10 \mu\text{m} < D < 100 \mu\text{m}$ ($30 < q < 300$).

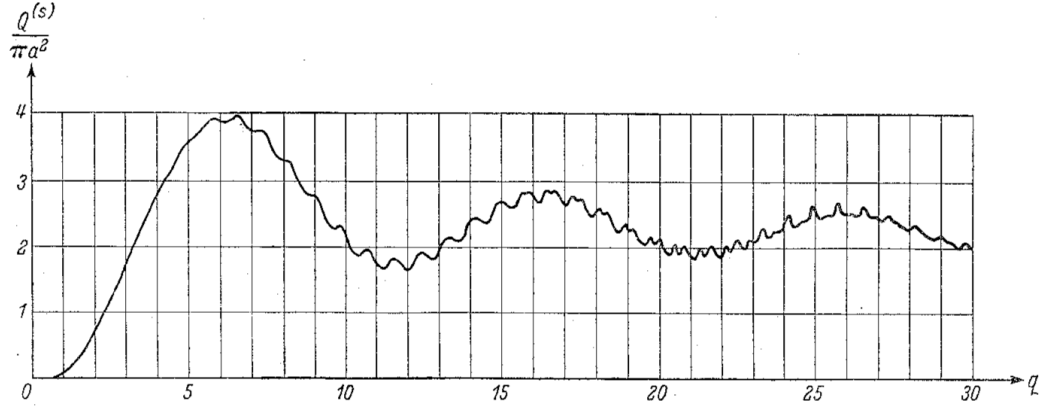


Fig. 13.14. The scattering cross-section of dielectric spheres of refractive index $n = 1.33$ as function of the parameter $q = 2\pi a/\lambda^{(1)}$.
(After B. GOLDBERG, *J. Opt. Soc. Amer.*, **43** (1953), 1221.)

Figure 1: Mie scattering cross-section, in terms of geometric cross-section, as a function of $q=2\pi a/\lambda$ (here $a = D/2 =$ particle radius). From Born & Wolf.

For our application, a simplifying limit is therefore reasonable. For large particles, the diffraction scattering cross-section converges to about twice the geometric cross-section¹, i.e.,

$$\sigma_{SC} \approx 2A = \frac{\pi D^2}{2} \quad (\pi D > \lambda).$$

In theory, the angular distribution of this scattered power is complicated, shifting from mostly forward at small diameters, to mostly backward at resonance ($\pi D/\lambda \sim 1$), and again to forward at large diameters (“bright dot in the shadow”). It further depends on particle refractive index and conductivity. However, situating the particle on a good mirror having a distinct index diminishes these variations. For purposes of estimating phase noise effects, we can take the scattered power to be roughly Lambertian in character, i.e.,

$$\begin{aligned} \frac{1}{P_{INC}} \frac{dP_{SC}(\theta)}{d\Omega} &\approx \frac{n_{\#} \langle \sigma_{SC} \rangle \cos \theta}{\pi} \\ &= 2F \cdot \frac{\cos \theta}{\pi} \end{aligned}$$

where P_{INC} is the incident beam power, dP_{SC} is the differential scattered power into solid angle element $d\Omega$ residing at co-latitude θ from the beam, $n_{\#}$ is the surface number density of particles, and $\langle \sigma_{SC} \rangle$ is the mean scattering cross-section per particle. In the second line we introduce the obscuration fraction F , the proportion of normal-projected

¹ Resonant peaks and valleys seen in Figure 1 will be washed out by integrating over a realistic distribution of random particle diameters.

surface area obscured by particles. Another way to look at this is that, independent of angular scatter distribution, the total hemispherical scatter is just $THS \approx 2F$.

Under similar assumptions, a large particle's absorption cross-section converges to just its geometrical area times the contaminant's effective albedo or emissivity ϵ ,

$$\sigma_A \approx \epsilon A = \epsilon \frac{\pi D^2}{4} \quad (\pi D > \lambda, 0 \leq \epsilon \leq 1).$$

The thermal absorption loss attributable to contaminant particles will then be

$$L_A^{dust} \equiv \frac{P_{ABS}}{P_{INC}} \approx \epsilon F$$

where P_{ABS} is the absorbed power. This power may be conducted into the substrate as heat or reradiated directly by the particle. Even with poor conductive contact, however, the mirror is expected to be a good radiative absorber (at acceptable particle blackbody temperatures). Radiative self-cooling of the particles is therefore unlikely to make a dramatic difference in the heat delivered to the substrate.

Functional limits for both effects depend on noise and loss budgets for AdL. As discussed in T070089, existing LIGO cavities show Lambertian scatter components of order 10 ppm per mirror. This level could degrade AdL phase noise, depending on how effective near-field light baffles are and how well they are isolated from mechanical vibration. As a result, our current AdL COC requirement (T080126) limits "point defect" and "small-scale topographic" scatter losses (those producing Lambertian-like flux distributions) each separately to less than 5 ppm per optic. To preserve this performance, particulate-generated $THS < 2$ ppm (i.e., $F < 1$ ppm) might be required over the lifetime of the interferometer.

Likewise, AdL performance at high power is likely to be limited by core optic absorption. T080126 requires absorption loss $L_A < 0.5$ ppm, but any improvement achieved by coating vendors will directly improve performance (and is therefore strongly encouraged). Limiting "acquired" contaminant absorption to $L_A^{dust} < 0.1$ ppm would appear prudent if it is feasible. Under the conservative assumption particles are "black" ($\epsilon \sim 1$), absorption would be the dominant driver for surface cleanliness.

Thermal decomposition of heated organic particles may deposit absorptive carbon films over areas exceeding the original particle's cross-section, perhaps even leading to thermal runaway. This is hard to predict without knowing the particle composition, but should be kept in mind as contamination sources and control methods are assessed.

Particle deposition rate

The obscuration fraction F for an optic in LIGO service should be straightforward, given environmental conditions over its history. Unfortunately, it is not.

The starting points for Weiss’ analysis T880049, and for most references in the space, military and optics literature, are Federal Standard 209 (*Airborne Particulate Cleanliness Classes in Cleanrooms and Clean Zones*) and MIL-STD-1246 (*Product Cleanliness Levels and Contamination Control Program*)². The processes connecting these two standards are complicated and model-dependent.

Fed-STD-209 parametrizes airborne particulates by Cleanroom Class *C*, which is proportional to volumetric particle number density $\rho_{\#}$. *C* is defined as the allowable number of particles per cubic foot of air exceeding $0.5 \mu\text{m}$ diameter, with limits for larger and smaller threshold diameters scaling as $D^{2.2}$. All classes have the same allowable size distribution, in principle differing only in scaled concentration³. Numerous authors suggest that, at least originally, the power law exponent of -2.2 was derived empirically from “typical” environments. It’s unclear how generally it applies to a given situation of interest.

Since the class levels are upper limits, it should be expected that actual densities in a cleanroom *rated* for a given class should be substantially lower under typical conditions.

Some subtlety arises in scaling deposition (“fallout”) rates from airborne particle concentrations. According to Tribble et al. (1996) and Hamberg (1982), the surface density of particles deposited from air at a given Cleanroom Class goes linearly with exposure time, but *not* with volume density of particles in the surrounding air. An empirical relation is given for particles larger than $5 \mu\text{m}$ (arguably our main concern, given the preceding):

$$n_{\#}(t) \approx 2.2 \times 10^5 \text{ m}^{-2} \cdot u \cdot b \cdot \left(\frac{t}{1 \text{ day}} \right) \left(\frac{C}{100} \right)^{0.773} \quad (D > 5\mu\text{m})$$

where $n_{\#}(t)$ is the surface number density of deposited particles, u and b are constants defined below, t is the exposure time and C is the cleanroom class.

The constant u accounts for the effect of air movement. It is assigned a value of 1 for still or slow-moving air, 0.1 for a typical cleanroom environment (about 10-15 air changes per hour), and 0.02 for a laminar flow airstream (nominal unobstructed air velocity 0.5 m/s or greater). The constant b accounts for surface orientation, with $b = 1$ corresponding to horizontal face-up (worst case), $b = 0.1$ corresponding to vertical (typical LIGO case), and $b = 0.01$ corresponding to horizontal face-down.

Presuming this holds for situations of interest, it would seem straightforward to bound F as a function of exposure time, orientation, and the airflow and environmental cleanroom class. Not so fast...

² Both standards have been rescinded in the last decade and “privatized” into equivalent ISO/IEC standards, but continue to be referenced.

³ Technically, the standard excuses small particles for dirtier classes, in apparent deference to measurement instrument limits.

Deposited particle size distribution

Surface fallout particle populations do not follow the parent airborne particle size distribution. One semi-empirical distribution of deposited particle sizes is embodied in MIL-STD-1246, which gives a recipe classifying all surfaces based upon a single “Particulate Cleanliness Level” or PCL. This represents that particle size (in μm) for which the mean surface number density of all particles that size and larger is less than one per square foot. Smaller particle sizes are assumed to follow a distribution asymptotically resembling log-normal, with a slope parameter ostensibly chosen to match empirical surveys. The number of particles per square foot exceeding a given diameter⁴ $x > 1 \mu\text{m}$ for given PCL = x_1 (in μm) is given in MIL-1246 as

$$\log(N(D > x)[\text{ft}^{-2}]) = 0.926(\log^2 x_1[\mu\text{m}] - \log^2 x[\mu\text{m}]) \quad (x > 1\mu\text{m}).$$

In a meta-analysis of samples from cleanrooms at NASA (Kennedy), Jet Propulsion Lab, TRW, Martin-Marietta, and The Aerospace Corporation, Hamberg and Shon (1984) find that this model does not accurately reflect actual contaminated surfaces. All surveys show a substantial excess of large particles, consistent with a much shallower slope parameter than MIL-1246 (a typical slope coefficient is found to be 0.383 rather than 0.926, using the same set of mixed units).

Evidently, the empirical data underlying MIL-1246 were developed by counting recently-cleaned surfaces. Cleaning processes preferentially remove larger particles, whereas any initial airborne population preferentially deposits its larger particles. One factor in this selection bias is that (for a given material density) larger particles have higher Stokes terminal velocity, and thus precipitate gravitationally more rapidly than smaller particles.

Hamberg and Shon present a theoretical model better matching the observed distributions. The model filters Fed 209-like airborne distributions according to the expected terminal velocity variation with particle size. They also demonstrate the preferential removal of large particles by solvent cleaning, showing that a steep MIL-1246-like spectrum is recovered after washing contaminated samples.

To explore implications (without artifacts from the $1 \mu\text{m}$ discontinuity) I generated normalized log-normal cumulative distributions asymptotically matching the MIL-1246 and Hamberg slopes (Figure 2). Weighting the corresponding differential probability densities by projected area per particle and integrating again numerically gives the cumulative obscuration contributed by particles up to a given diameter (Figure 3)⁵.

⁴ The standard says nothing (indeed, the formula gives nonsensical negative densities) for particles smaller than $1 \mu\text{m}$.

⁵ A more general semi-analytic approach is given by Barengoltz (1986).

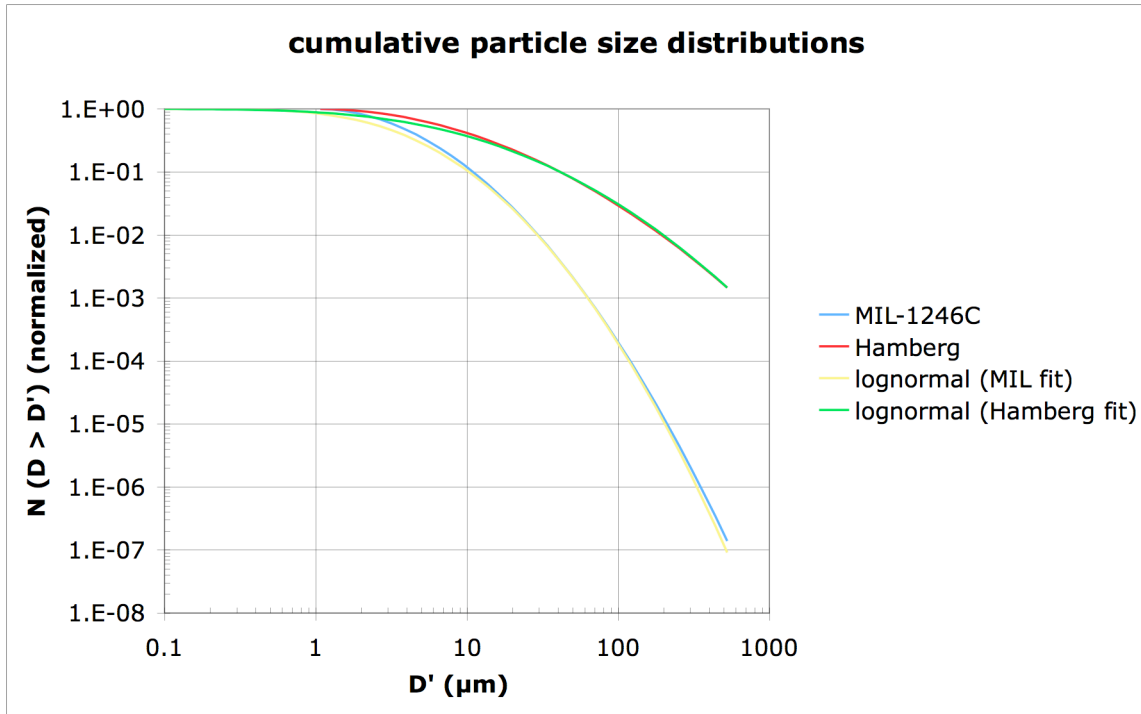


Figure 2: Normalized cumulative distribution of particle sizes on cleanroom-exposed surfaces, according to Hamberg and Shon (1984) and MIL-STD-1246C. Log-normal fits were created to extend the models below 1 μm (see text).

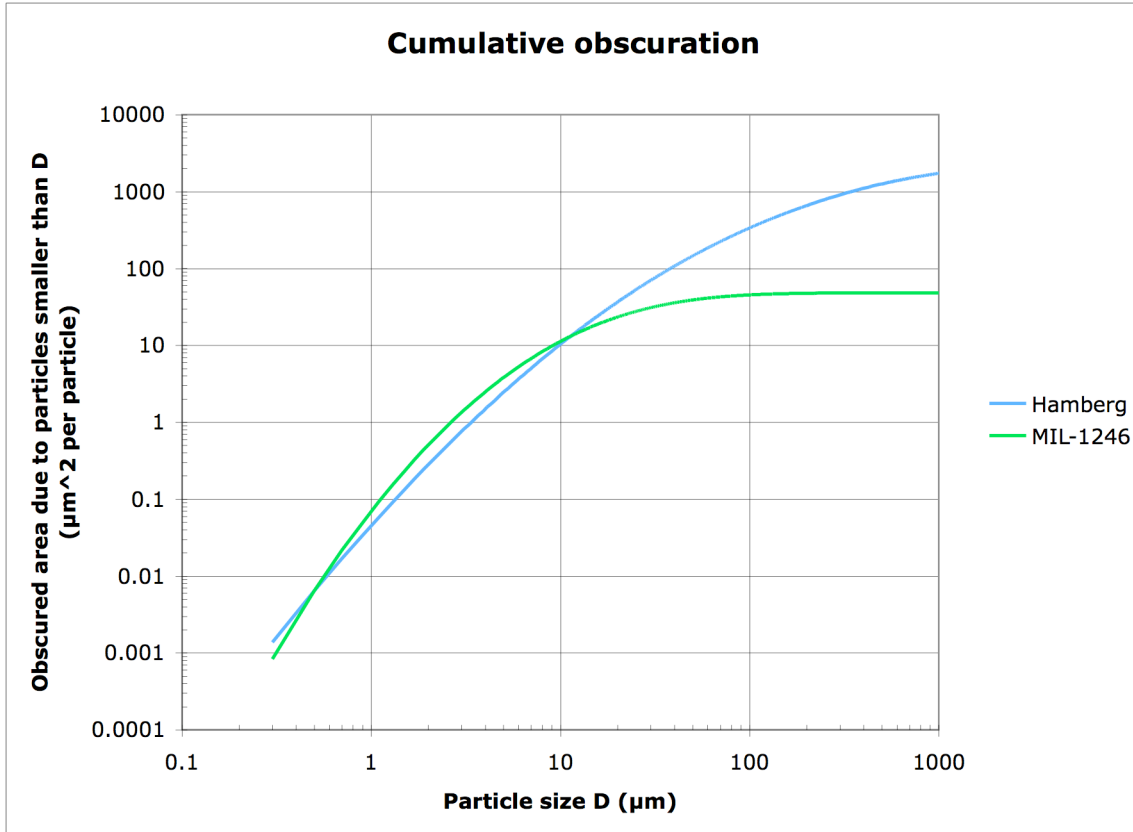


Figure 3: Cumulative obscuration by populations distributed according to MIL-1246 and Hamberg models, normalized to the same total number of particles.

For the steep MIL-1246 size spectrum, the obscuration ratio F is essentially determined by the number of particles between about 5 and 100 μm diameters. With the more realistic observed spectrum, however, significant obscuration continues to accrue up to very large particle diameters, unless there is some cutoff applied.

In this connection Hamberg and Shon remark “Typically, the upper limit of particle sizes found in clean room air is approximately 200 μm .” However, NASA and Aerospace Corp. data presented in that same paper show significant counts out to 1,000 μm , with no evident change in slope.

Some kind of cutoff must apply, of course. At the least, dust bigger than several mm will attract scrutiny and (if accessible) be cleaned off. One also expects a window function, rather than a diverging bias, from the terminal velocity effect; very large particles should drop from the air stream en route before they can reach the target. This will introduce a cutoff dependent on “source proximity,” entrainment time, or cleanroom size. For the same reason they are easier to wash off, large particles will also spontaneously blow, roll or fall off the surface more readily.

Finally, according to the definitions adopted in Fed 209 and MIL-1246, narrow fiber-like or needle-like particles are to be binned according to length, potentially biasing area estimates based on assumed spherical shape. Barengoltz (1986) offers an adaptation to account for this if, for example, contaminants are known to be primarily fibrous.

In what follows I'll artificially take 200 μm as a sharp cutoff to the spectrum. It bears emphasis, however, that large particles *do* occur in good cleanrooms, and in LIGO⁶. A few outliers can dominate the occluded area. Furthermore, their absorption will be spatially localized compared to an area-equivalent statistical population of smaller absorbers. This potentially complicates thermal figure error compensation.

Acquired surface obscuration fraction

To estimate integrated surface obscuration after a period of environmental exposure, the above expression for $n_{\#}$ ($D > 5 \mu\text{m}$) is first corrected to include particles smaller than 5 μm . 34% and 64% of particles were found to be larger than 5 μm for MIL-1246 and Hamberg distributions, respectively, so correcting for the full range of particle sizes gives

$$n_{\#}(t) \approx \left\{ \begin{array}{l} 6.5 \\ 3.4 \end{array} \right\} \times 10^5 \text{ m}^{-2} \cdot u \cdot b \cdot \left(\frac{t}{1 \text{ day}} \right) \left(\frac{C}{100} \right)^{0.773} \left\{ \begin{array}{l} \text{MIL-1246} \\ \text{Hamberg} \end{array} \right\}.$$

The corresponding mean area per particle derived above is 48 (μm)² for the MIL spectrum and 655 (μm)² for Hamberg (again, using an artificial 200 μm maximum diameter cut). Therefore

$$F(t) = n_{\#}(t) \cdot \left\langle \frac{\pi D^2}{4} \right\rangle \approx \left\{ \begin{array}{l} 31 \\ 225 \end{array} \right\} \times 10^{-6} \cdot u \cdot b \cdot \left(\frac{t}{1 \text{ day}} \right) \left(\frac{C}{100} \right)^{0.773} \left\{ \begin{array}{l} \text{MIL-1246} \\ \text{Hamberg} \end{array} \right\}.$$

For example, this predicts a mirror hanging vertically ($b = 0.1$) in still air ($u = 1$) at Class 100 particle concentration could acquire 0.1 ppm absorption (for particulate $\epsilon = 1$) in about 6 minutes. Aggressive laminar flow ($u = 0.02$) at the same ambient concentration extends the allowable exposure to about 5 hours; simultaneously reducing the concentration to the equivalent of Class 10 brings it to 32 hours.

Tribble et al. (1996) assigns 95% confidence intervals to calculations of this type at *one order of magnitude in each direction*.

⁶ In G080078 (page 6) there is a picture of the H2 ETMy on resonance. An extended scattering source, evidently fully resolved, looks to be about 1 mm across (from the scaled beam waist). Several other resolved scatterers on this mirror appear to be at least half this size.

3. Particulate contamination sources

VEA/LVEA and softwall cleanrooms

We get good particle counts (better than 3500 m^{-3} , our initial spec) holding a counter still at shoulder height inside the softwall cleanrooms. However the condition of the VEA floor, sealing around vacuum penetrations, seismic supports, cable trays and piping will be defeating the purpose for “real” operations, by generating eddies, harboring dirt and releasing it when people move around.

These are textbook dirt traps, probably not “cleanable” in any operationally useful sense. Deinstalling cabling and piping isn’t an option, since instrumentation has to be operational for core optic integration. Covering or isolating them seem the best options.

It probably makes sense to subdivide processes which require “large aperture” access (parting the 104” BSC domes, multiple BSC or HAM door removal, VE section rearrangement) from those which only require a single entry/egress.

For the former, we can perhaps consider using existing cleanroom systems with some adjustments to improve sealing and curtain gap closures. For example, we can lay sheeting over the trays and contaminated floor areas underneath to limit communication with the cleanroom flow. We could supplement this by remediative vacuum cleaning of exposed volumes after incursions (presumably early ones, preceding introduction of most optics).

For small “one-door” access episodes, e.g., the final release/adjustment/cleaning of core optics, we can amplify the current practice of sealing a small cleanroom around just the access door and immediate area, thereby excluding cable trays, piping, HEPI actuators, and other ancillary equipment. Sealing a “boot” or tunnel to the HAM or BSC flange immediately after door removal should be fairly effective. We should strive to maintain a curtain gap at floor level consistent with unidirectional outward flow (total vent area comparable to or smaller than the active blower area in the ceilings).

We especially need intermediate gowning rooms and equipment prep areas of adequate size and air flow, *in addition* to the laminar flow clean room protecting the chamber entry.

Clean air purge system

Our clean air skirts normally produce zero particles above 0.3 microns when measured in the outlet nozzle (typical sensitivity threshold is ~ 350 per cubic meter)⁷. However, measurements just inside the chamber inlet sometimes yield much higher counts,⁸

⁷ Harry Overmier (p.c., January 2008)

⁸ R. Schofield, LHO ilog 12/20/2007, http://ilog.ligo-wa.caltech.edu/ilog/pub/ilog.cgi?group=detector&date_to_view=12/20/2007&anchor_to_scroll_t

possibly implying contamination of the supply piping. Our standard vent practice is to spin up the compressor skid and purge the lines at full flow, by temporarily parting the last flanged joint before the repress valve. This leaves a small unpurged dead space within the valve itself, but it's difficult to understand how this small volume, fully sealed between vents, could acquire and harbor significant contamination.

Given the likely influence of static charge in the sticking probability, it would be good to investigate means for increasing the conductivity of purge gas without adding humidity or net charge (which could backfire). Radioactive polonium flow ionizers might be one option.

Vacuum envelope walls

In addition to particles carried in on equipment, personnel and the purge air, we appear to also have contamination “generated” (or harbored) by the internal oxide layer on most the vacuum vessel surfaces. Schofield generated a particle plume with peak density exceeding 3×10^6 particles per cubic meter by brushing against the oxidized wall of the Hanford corner volume.⁹ A non-oxidized zone was a factor of five less active, but still yielded a measurable plume.

This dust has evidently also built up a substantial reservoir on the floor of all the chambers, which is stirred up by human activity and may be transported by pumping, venting and purge airflow. A thorough cleaning of the vacuum envelopes appears essential before starting AdL installation. We need to develop a feasible and effective process.

Personnel

People stir up the accumulated dirt in the chambers and also emit particles, even when properly garbed. Design guidelines vary on how much direct particulate generation to expect from workers, depending on garb type, garb history (number of washing cycles is a large factor), donning environment and technique, and the nature of the work activity. Flomerics Inc. used the figure of 3,950 particles/second greater than $0.5 \mu\text{m}$ per worker in their BSC study commissioned by LIGO in August 2006.¹⁰

The resulting particle density at a nearby target point depends on the diffusion mechanism. For example, our typical corner purge volume flow is about $0.1 \text{ m}^3/\text{s}$ (see below). The Flomerics model worker intercepting this flow can induce a downwind concentration of $80,000 \text{ m}^{-3}$. (class ISO-6 or -7, Fed 209E class 5,000).

[o=2007:12:20:18:25:54-robert](#)

⁹ Schofield, *loc. cit.*

¹⁰ Flomerics Inc., *Contamination Control Study: BSC Chamber*, LIGO-T060205-00-D (8/14/2006). Primary source cited therein: *People as a Contamination Source* by Ljungqvist and Reinmuller (?).

Shortly after a substantial incursion at LHO (two to four people working in two internal locations for most of a shift) Schofield¹¹ measured ambient levels of order 35,000 m⁻³ (again, greater than 0.5 micron diameter). After 12 hours, no particles were detected (at minimum resolution ~ 350 m⁻³) A very brief “inspection” incursion by one worker then generated about 3,500 m⁻³ concentration.

Equipment

Presuming we take available precautions against carrying in or emitting dust from our bodies, there remains the danger of generating particulates inside during assembly and adjustment. Gustafson and Lazzarini’s trip report¹² highlights significant losses at NIF caused by “large” particles shed by fasteners, sliding contacts and adjustment mechanisms. Indeed, Schofield¹³ found similar “mechanical” detritus in his LHO inspection, and Vorvick and Garofoli noted visible dust collected on the LOS structures. The latter appeared to be silver plating shed by earthquake stop screws¹⁴, which are readjusted each time there is work done in the chamber.

Large particles and shards (10-1000 μm) evade airborne sampling, but may be sufficiently mobile to reach and stick to optics.

Earthquake stops, flexure clamps, and safety screws that are turned to free or adjust unprotected optics are especially worrisome. Silver plating should *not* be used to prevent galling on adjustment or multiple-use fastening screws, or on sliding parts. Instead, bearing-compatible base metals should be chosen for mating components. The ELI earthquake stop retrofit is having good results with precipitation-hardened beryllium copper screws running in 304 stainless steel, for example.

Open hatches and doors

There is apparently significant exchange of air through open chamber doors (qualitatively much stronger than the deliberate purge flow, for example). This is probably driven by turbulence in the external softwall cleanroom, which maintain strong vertical flow (0.5 to 1.5 m/s velocity) outside. Schofield’s measurements just outside the chamber verified that the exterior space was significantly cleaner than the work zone within the chamber. With appropriate measures to improve the performance and coverage of the cleanrooms, this ambient air should be even cleaner. However curtains are often drawn across the opening after equipment and people are inside, to reduce turbulence for critical operations.

¹¹ Schofield, *loc. cit.*

¹² Gustafson and Lazzarini, “Visit to NIF in Livermore,” LIGO-T080031 (2/12/2008).

¹³ Schofield, *loc. cit.*

¹⁴ Vorvick, LHO ilog 12/19/2007, http://ilog.ligo-wa.caltech.edu/ilog/pub/ilog.cgi?group=detector&date_to_view=12/19/2007&anchor_to_scroll_to=2007:12:19:12:09:11-Vorvick

4. Operational & process requirements

Assembly

We will protect the optic surfaces and handle the assemblies under Class 100 conditions up to the moment they are integrated in the vacuum envelope. Since shielding and final in-situ cleaning will be employed, we should focus on preventing contamination from hitching a ride into the vacuum envelope on surfaces and tooling.

For example I notice we aren't being all that serious about double- and triple-bagging; an outer bag that has traveled far and wide is often brought *inside* the sterile assembly area, distributing whatever's accumulated on its surface, before removal. Similarly, I see foil packets reused repeatedly, the parts inside gradually getting covered with aluminum shreds.

I suggest adopting some of the process guidelines provided by NIF¹⁵, e.g.,

- hard containers for all small parts and fasteners
- clear away and discard packaging, used gloves and debris immediately
- remove & discard outer packaging & vacuum off inner packaging in gowning room/antechamber.
- provide adequate gowning room/antechamber in the first place (incl. a place to decontaminate hardware outer packaging)
- periodically wipe down and vacuum clean the assembly area to deplete particulates at their source

Installation

Assuming we directly shield active optic surfaces up to and during the actual installation process, the emphasis continues to be collecting and removing dust as it is acquired. Assemblies should be transported and staged entirely within clean environments, and lift fixtures and crane penetrations should be properly sealed.

Final alignment & test

The final stage in installing suspended optics involves people working inside to:

- connect and test or fine-tune OSEMS, clearances and gaps
- adjust equilibrium alignment to optical fiducials
- clean the optic surface
- remove tooling and seal the chamber

The optic needs to function dynamically and optically for some of these processes, certainly at the end, so any conformal coating or other protection will be removed. As a result the unprotected optic can be subjected to direct dust generation (from the people working on it) for at least part of the time.

¹⁵ Gustafson and Lazzarini, "Visit to NIF in Livermore," LIGO-T080031 (2/12/2008).

Based on the AdL suspension geometry, most of the work will be done by one or two pairs of gloved hands, directly above the suspended optic or at the level of the intermediate masses 30 to 150 cm above the optic. Typically the hands are manipulating threaded fasteners and adjusting screws, connecting or dressing wiring, or checking gaps with feeler gauges.

We have found that initial LIGO core optic alignment can be hampered by small amounts of air flow. The most extreme interaction is with the mode cleaner cavities, probably because the IO purge inlet is very close to MC2. However fine-adjusting the core optic PAM magnets or OSEMs is also impossible unless the corresponding section's purge is either cut off entirely, or throttled back to a small fraction (backfill angle valve cracked open ½ turn or so, perhaps 5% of maximum in terms of volume flow rate)¹⁶.

The aerodynamic drag force F on an object of cross section $A = \pi d^2/4$ will scale as

$$F \approx \frac{1}{2} \rho v^2 \cdot A \cdot C_D \approx 0.2 \text{ N} \cdot \left(\frac{v}{1 \text{ m/s}} \right)^2 \left(\frac{d}{0.3 \text{ m}} \right)^2 \left(\frac{C_D}{1} \right)$$

where C_D is the coefficient of drag, of order unity for a cylinder¹⁷, and $\rho \sim 1.2 \text{ kg/m}^3$ is the density of air. Flow velocities below about 0.2 m/s are generally not considered useful for particulate control where people are working, or where obstacles interrupt the flow¹⁸. As a result, we expect about 10 mN of aerodynamic drag from a minimally effective laminar flow system.

Even if steady in the far field, such a flow will induce fluctuating torques on the mirror through wake vortex shedding. A cylindrical obstacle begins creating vortices at Reynolds numbers above about 30¹⁹; at 0.2 m/s air velocity, our test mass has $R_e \sim 5,000$. The simplest (lowest-velocity) vortex shedding pattern causes the effective center of pressure to wobble back and forth with respect to the center of lateral area, with excursions comparable to the body radius (falling leaf effect). As a result, fluctuating torques from the wind can be of order the full aerodynamic drag force divided by the mirror radius. As velocity rises, the individual vortex size and characteristic timescale diminish, but the driving force increases roughly as the square of the velocity.

¹⁶ Gary Traylor, Betsy Bland, Cheryl Vorvick, (p.c., March 12, 2008)

¹⁷ for Reynolds numbers in the range $100 < R_e < 10^5$, spanning the plausible range of our application; cf. Fig. 2 in “Drag of Blunt Bodies and Streamlined Bodies,” http://www.princeton.edu/~asmits/Bicycle_web/blunt.html, or Fig. 3 in Wang et al, “Prediction of high Reynolds number flow over a circular cylinder using LES with wall modeling,” <http://ctr.stanford.edu/ResBriefs01/wang.pdf>

¹⁸ W. Whitfield (inventor of the laminar flow clean room and bench), quoted in “Profile of Willis Whitfield,” *The Cleanroom Monitor* no. 47 (Scottish Society for Contamination Control, August 2003)

¹⁹ Tritton, D.J., *Physical Fluid Dynamics* (Van Nostrand, 1977).

A practical airflow system would thus be ineffective for dust control unless we can operationally tolerate tens of mN of aerodynamic force, and several mN-m of fluctuating torque during installation. If final alignment processes demand still air, as they do for initial LIGO, the optic will be unprotected at precisely the times it is most vulnerable (people working directly on or above it, with no shield on the coating).

Irrespective of fine alignment, for general operations it will be necessary to leave the optic hanging free much of the time without locking its earthquake stops. It is important to verify that a free-swinging optic (perhaps one with failed electronic damping) will not be damaged by aerodynamic buffeting. Since air and structure motions associated with people working nearby would presumably be comparable or worse, this may not be a significant worry.

The corner station purge air system (see below) running full bore is capable of pushing air through a BSC or HAM nozzle no faster than about 0.015 m/s. This is of order one thirtieth the speed required for minimal “laminar flow” type dust control. As noted, however, it seems to clean up the environment after a disturbance, given some hours settling time.

Even if there is no need for “quiet time” where we are forced expose the optic to dust without flow protection, we will probably rely at least to some degree on cleaning the mirror as non-invasively as possible just before evacuation. Reapplication of “First Contact” or drag wiping require significant handling and a lengthy incursion. The air knife system developed at Livermore²⁰ should be investigated as an alternative for minimally-invasive “last licks” touchup.

Maintenance, repairs and other non-alignment access

COC/SUS installation is merely the first of many access episodes. Repairs, inspections, and incursions to work on unrelated components will be more numerous over the life of the apparatus. It’s important not to require extensive subsets of the initial build procedure in every incursion.

For example, we prefer to have the option to forego re-cleaning mirrors with every vent or incursion. An incursion just to fix an internal feedthrough connector might nominally be feasible for a single worker in a few minutes. Mirror cleaning, if also mandated, might consume an entire shift, compound ambient contamination (by forcing two or more people to work inside for ~ hours), and incur damage risk. In the corner stations, a large number of optics would presumably have to be cleaned.

Pumpdown & backfill

Whether we keep the mirrors pristine or rely on “final cleaning” to erase contamination, the key question is whether they stay clean after we close up. Subsequent particle mobility is a potential problem. Initial LIGO experience suggests it is happening, at least to some degree; LIGO core optics drag-wiped years ago are later found to have acquired

²⁰ Gustafson, *loc. cit.*

constellations of “new” dust particles. Understanding this is potentially critical for Advanced LIGO.

We’ve made some attempts to understand if dust migrates when the doors are on (e.g., witness plates), but have no systematically believable results yet. New witness plates were recently installed near accessible view ports, to look for acquired contamination from the outside, and thereby separate pumpout effects from those due to backfilling.

One favorite theory is that pumping and/or backfill generate turbulent flow, which entrains and transports particles from the envelope walls or trapped in crevices. The corner station clean air skids are rated for 200 scfm, or about 0.1 m³/s volume flow²¹. Worden²² estimates that header and valve conductance limits the actual achieved flow at the chamber inlets to perhaps ¼ of this. This is coincidentally about the same volume rate as a QDP80 roughing pump (43 cfm). QDP80’s are generally deployed in pairs for roughing at LLO²³, but header conduction losses probably limit the net flow. Representative nozzle velocities and Reynolds numbers (diameter-referred) are as follows.

Tube (diameter)	R_e (@ dia.)	v (m/s)
Header (6’’)	15,000	1.4
MC tube (30’’)	2,500	0.05
BSC nozzle (60’’)	1,500	.015

Table 1: Air velocities and Reynolds numbers for volume flow of 0.025 m³/s, corresponding to typical purge or roughing with a QDP80 pump.

The nominal threshold for onset of turbulence in tube flow is around $R_e \sim 2,300$ ²⁴. In the chambers and larger tubes, we’re indeed near or above the turbulence transition with maximum available flows, though not by a huge factor.

Accepting some operational inconvenience, we could throttle the pumpdown or backfill during the viscous flow phase. Typically most of the time to operation is devoted to degassing water vapor in molecular flow anyway, so there is no rush for typical pumpdowns (the notable exception being “crash dives” to fix hangups during a science run). A factor of 2-5 increase in roughing or vent time could insure most flow was laminar (except perhaps within the inlet/outlet nozzle). It may in fact only be necessary to throttle while pressure is close to atmospheric.

For backfill, we could also consider installing flow diffusers on repress nozzles to encourage the transition to laminar flow. Doing so could make the inlet harder to keep

²¹ End stations are equipped with 50 scfm capacity units, or .025 m³/s

²² p.c., 3/13/08

²³ At LHO we still use the Roots blowers for roughing sometimes, but they aren’t strictly needed.

²⁴ Tritton, *loc. cit.*

clean, however. For pumpdown, it's irrelevant if turbulence starts near the outlet; anything entrained there is heading the right way.

Another theory is that shock and vibration associated with parting or reinstalling the large doors, and/or initial personnel entry, releases cascades of particles. This seems plausible given Schofield's findings on loose oxide. Transient airflow through the fresh opening may also play a role. A means to protect the optics during the critical entry and exit transitions, before establishing steady-state conditions, could be advantageous.

In theory, there could also be particulate migration under vacuum (e.g., particles falling from above optically "trapped" by the laser beam, or attracted electrostatically; or ballistic particles propelled by acoustic or thermal events at the walls).

5. Design criteria and sample flow system concept

Even presuming we develop reliable in-situ cleaning and have no vent/purge migration, there still may be a need for some kind of practical blanket protection. The foregoing considerations, taken with some rudimentary clean room design rules^{25,26}, give essential criteria for such a system:

- The system should provide standard clean bench face velocities (say between 0.5 and 2 m/s). Variable airflow might be helpful for special situations (e.g., acoustic or vibration sensitivity, rapid blowdown after a disturbance), but the system can't be effective at very low speeds.
- The flow should encounter no obstructions upstream of the optic.
- The flow should not direct contamination from known particulate hotspots or people toward the optic.
- The flow should preferentially establish a shear boundary in the plane of the optic coatings.
- If possible, terminal diffuser and collector equipment and internal ducts should be fixed, UHV- compatible, and geometrically unintrusive, such that no chamber incursion is required to start up or shut down. This affords potential for continuous protection through entry and egress transients.
- The equipment should be economical so each core optic can be provided with its own; in general, all the optics in a given volume would usually want protection at the same time.
- The equipment should *not* be mechanically coupled (through ducting, electrical lines, or supports) to isolated seismic platforms.

These criteria suggest a vessel-mounted diffuser and collector system, blowing *upward* or *sideways* (*horizontally*). Aerodynamic obstructions everywhere above the mirror, and

²⁵ Baker Analytical, *Intro to Clean Benches*, http://mems.sandia.gov/ua/device-doc/equipment/Supporting Documents/Education and Resources_Intro to Clean Benches.pdf

²⁶ Whitfield, *loc. cit.*

predominance of overhead particle generation (from manual work on upper SUS and SEI stages), effectively preclude downflow options.

While an upward flow configuration looks mechanically simple at the diffuser end, good eddy control and closure of streamlines argue for a simplified path to the collector, which is not practical overhead. Also, the turbulent “wake” of the optic will tend to entrain and collect particles. If the wake streams upward, they can settle out on the mirror or on higher surfaces, rather than fall to the chamber floor.

As a result, a simple side-flow system (Figure 1) seems a good compromise. A UHV-compatible diffuser panel would be mounted to blow horizontally through the suspension. The panel is independently supported by the BSC or HAM vessel wall, and is ducted to a fixed conflat port on the vessel body (e.g., a “G” waist nozzle on the BSC, or the overhead “Air Shower” nozzle on the HAM). External blower/filter units, which may be portable, can be connected to the outside of these flanges with flexible ducting. These may also incorporate electrostatic charge neutralization. Provisions for initial blowdown and purge sampling are made at the supply connection.

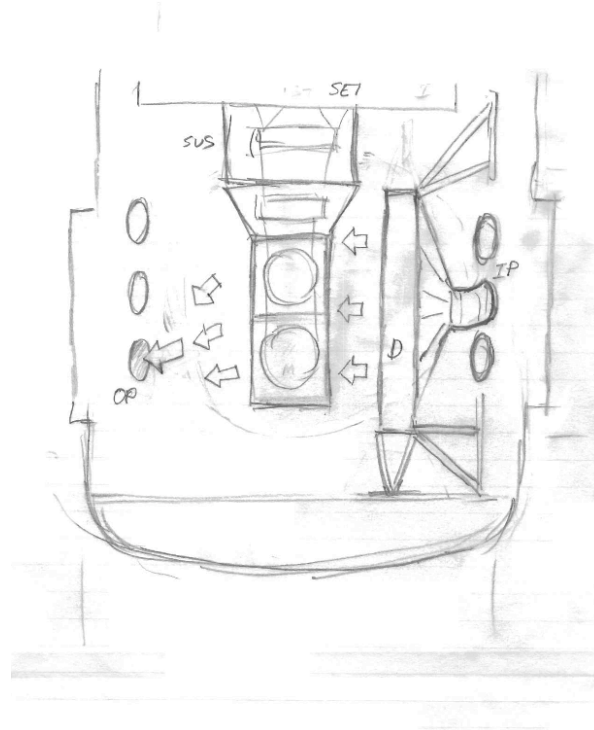


Figure 4: Laminar flow COC dust protection concept (configured for BSC application). An external blower/ULPA filter unit (not shown) pushes filtered air from outlet port *OP* to inlet port *IP*. This is ducted to laminar-flow diffuser *D*, which is supported by struts from internal chamber hard points. Gate valves or blank flanges mounted outside *IP* and *OP* seal the chamber for vacuum service; the diffuser and internal ductwork are UHV-compatible, and remain inside.

Gate valves to isolate supply and return ports for vacuum service would be most convenient for cycle speed and cleanliness, but potentially costly for large apertures. As a fallback, ports could be normally blanked off, and only fitted with duct nozzles after volume backfill. Existing vent/purge systems give adequate outward flow for removal and replacement of small (~10") covers without risking internal contamination. We rely on this for servicing viewports and feedthroughs.

A symmetrically placed collector panel would improve streamline uniformity and robustness for a given diffuser area. Making the diffuser larger, and situating it as close as possible to the suspension, could achieve comparable effect without blocking access to both sides. If no explicit collector is used, air can be returned through any convenient port or ports, preferably situated approximately opposite the diffuser.

Ideally the diffuser panel's width and height would be substantially greater than its distance from the payload. Actual choice of dimensions will involve a compromise between cost, access, total flow rate, and other space requirements, including oblique camera views, neighboring optics, and beam paths. Maintaining adequate face velocity will require correspondingly higher velocities in the ducting, so portions of the system (including the filter units) will be pressurized.

An affordable configuration applicable to all required chamber geometries may present other design challenges, but the proposed concept is modular and mostly decoupled from other subsystems. Ideally, external hardware could be COTS, and only internal diffusers, ducts and supports would require custom fabrication.

In the best case, efficient cleaning, charge control, and a clever alignment or operations strategy might obviate the need for an airflow apparatus. No matter how simply we can devise such a system, it's worth hard consideration if it can be avoided entirely.

6. Appendix: scattering and absorption from particulate contaminants

7. Appendix: Expected and observed distributions of particle sizes

8. References

Weiss, R., *Dust accumulation on optics, scattering and requirements on clean area for the LIGO*. LIGO-T880049 (December 1988).

Fritschel, P. and Zucker, M., *Wide angle scatter from LIGO arm cavities*. LIGO-T070089 (May 2007).

Billingsley, G., Harry, G., Kells, W., *Advanced LIGO Core Optics Components Design Requirements Document*. LIGO-T080026 (February 2008).

Tribble, A.C., Boyadjian, B., Davis, J., Haffner, J. and McCullough, E., *Contamination Control Engineering Design Guidelines for the Aerospace Community*. NASA Contractor Report 4740. Rockwell International Corp., Downey, CA (May 1996).

Hamberg, O., "Particulate fallout predictions for clean rooms." *J. Env. Sci.* **25**(3) p. 15 (1982).

Hamberg, O. and Shon, E.M., *Particle Size Distribution on Surfaces in Clean Rooms*. U.S. Air Force Systems Command Space Division Report SD-TR-84-34. The Aerospace Corporation, El Segundo CA (30 April 1984).

Hubbard, R., *M1 Microroughness and Dust Contamination*. Advanced Technology Solar Telescope Technical Note No. 0013 rev. C. ATST, Tucson AZ (28 October 2002).

Barengoltz, J. B., "Calculating the Obscuration Ratio due to Particle Surface Contamination," *J. Env. Sci.* **29** (6) p.36 (November-December 1986).

Barengoltz, J. B., "Calculating Obscuration Ratios of Contaminated Surfaces," *NASA Tech. Briefs*, Vol. 13, No. 8, Item 2 (August 1989).

Tveekrem, J., *Contamination Effects on EUV Optics*, NASA/TP-1999-209264. Marshall Spaceflight Center, Huntsville (June 1999).

NASA Occupational Safety and Quality Assurance Branch, *Contamination control requirements manual*, publication JPG 5322.1 rev. E. Johnson Space Center, Houston

(November 2000).

Ma, P. T., Fong, M. C., and Lee, A. L., “Surface Particle Obscuration and BRDF Predictions,” SPIE Vol. 1165, *Scatter from Optical Components*, pp. 381 - 391 (1989).

Jillavenkatesa, A., Dapkunas, S.J., and Lum, L.S.H., *Particle Size Characterization*. NIST Recommended Practice Guide, Special Publication 960-1. U.S. National Institute of Standards and Technology (January 2001)

Spyak, P.R. and Wolfe, W.L., “Scatter from particulate-contaminated mirrors. Part 1: theory and experiment for polystyrene spheres and $\lambda=0.6328 \mu\text{m}$ ” *Opt. eng.* **31**(8), p. 1746 (August 1992).

Spyak, P.R. and Wolfe, W.L., “Scatter from particulate-contaminated mirrors. Part 2: theory and experiment for dust and $\lambda=0.6328 \mu\text{m}$ ” *Opt. eng.* **31**(8), p. 1757 (August 1992).

Spyak, P.R. and Wolfe, W.L., “Scatter from particulate-contaminated mirrors. Part 4: properties of scatter from dust for visible and infrared wavelengths” *Opt. eng.* **31**(8), p. 1757 (August 1992).

Young, R.P., “Mirror scatter degradation by particulate contamination.” SPIE Vol. 1329, *Optical System Contamination: Effects, Measurement Control II*, p. 246 (1990).

Kells, W. P., *Interpretation of OTF Scatter Loss Scans*. LIGO-T080010-01-D (2 April 2008).

Kells, W. and Vorvick, C., *Imaged scattered light from LIGO resonant cavities: micro-roughness vs. point scatter loss*. LIGO-G080078-01-D (20 March 2008).

Stover, J. C., *Optical Scattering – Measurement and Analysis*, 2nd ed. SPIE Press, Bellingham, WA (1995).

van de Hulst, H. C., *Light Scattering by Small Particles*. Wiley, New York (1957).

MIL-STD-1246C, *Product Cleanliness Levels and Contamination Control Program*. U.S. Army Missile Command, Redstone Arsenal, Alabama (April 1994).

FED-STD-209E, *Airborne Particulate Cleanliness Classes in Cleanrooms and Clean Zones*. U.S. General Services Administration and Institute of Environmental Sciences, Mount Prospect, IL (September 1992).

Born, M. and Wolf, E., *Principles of Optics*, 2nd ed. Pergamon, New York (1964).

Jackson, J.D., *Classical Electrodynamics*. Wiley, New York (1962).